

Simulations of underwater plumes of dissolved oil in the Gulf of Mexico

Alistair Adcroft^{1,2}, Robert Hallberg^{2,3}, John P. Dunne², Bonita L. Samuels²,
J.A. Galt⁴, Christopher H. Barker⁴ and Debra Payton⁴

Accepted for publication in Geophysical Research Letters Copyright 2010 American Geophysical Union. Further reproduction or electronic distribution is not permitted. The correct citation for this article is:

Adcroft, A., R. Hallberg, J. P. Dunne, B. L. Samuels, J. A. Galt, C. H. Barker, and D. Payton (2010), Simulations of underwater plumes of dissolved oil in the Gulf of Mexico, *Geophys. Res. Lett.*, doi:10.1029/2010GL044689, in press.

Abstract

A simple model of the temperature-dependent biological decay of dissolved oil is embedded in an ocean-climate model and used to simulate underwater plumes of dissolved and suspended oil originating from a point source in the northern Gulf of Mexico, with an upper-bound supply rate estimated from the contemporary analysis of the *Deepwater Horizon* blowout. The behavior of plumes at different depths is found to be determined by the combination of sheared current strength and the vertical profile of decay rate. For all plume scenarios, toxic levels of dissolved oil remain confined to the northern Gulf of Mexico, and abate within weeks after the spill stops. An estimate of oxygen consumption due to microbial oxidation of hydrocarbons suggests that a deep plume of hydrocarbons could lead to localized regions of prolonged hypoxia near the source, but only when oxidation of methane is included.

¹Princeton University, Program in Atmospheric and Oceanic Sciences, 300 Forrester Rd., Sayre Hall, Princeton, NJ 08540-6654 email: adcroft@princeton.edu

²NOAA Geophysical Fluid Dynamics Laboratory, 201 Forrester Rd., Princeton, NJ 08540-6654

³email: Robert.Hallberg@noaa.gov

⁴NOAA Office of Response and Restoration, 7600 Sand Point Way NE, Seattle, WA 98115-6349

Introduction

Since the explosion of the Deepwater Horizon (hereafter DWH) drilling platform on 20 April 2010, there has understandably been much media and academic attention on the surface expression of the resultant oil leak (which continues at the time of writing). This spill is the largest in U.S. history and the ensuing environmental impact may be unprecedented. In addition to the very visible surface slick, there has been concern raised about the appearance of underwater, horizontally extended, plumes of dissolved oil. In particular, there is evidence that a fairly contiguous deep plume formed approximately 200-500 m above the ~1500 m deep well-head [JAG, 2010].

There are extensive resources and experience in forecasting the propagation of a surface oil slick and projecting the consequences [NRC, 2002]. There is comparatively less experience in forecasting the evolution of spilled oil from deep leaks. A deep oil leak, ejected under pressure, may form an entraining, vertical plume of oil, gas, hydrates and ambient water (see Fig. 1 in the supplemental material). The plume is buoyant so long as there are large volumes of oil and gas in the mix, but may reach a terminal layer in which the upward motion is substantially reduced. This transition may be triggered, for example, by the dissolution of methane at high pressures, thereby removing one source of buoyancy from the plume. Beyond the transition layer, the larger droplets rise at their terminal individual velocities and ultimately make it to the surface, providing the material to form the surface slick. The more soluble compounds within the oil may dissolve, particularly from small droplets that are prevalent in the vertical plume, where the vigorous turbulence gives rise to small droplet sizes. Subsea injection of dispersants will also create tiny droplets and encourage dissolution of oil [NRC, 2005]. There is large uncertainty in the proportion of material that remains within the water column, at what depths, and in what form. Small enough droplets ($< \sim 100 \mu\text{m}$ diameter) and the dissolved components are retained in the water column, and can for the most part be considered dynamically passive and neutrally buoyant, at least on time-scales of days to weeks. Tentative observations suggest that a measurable amount is retained at depth and has formed horizontally extended plumes [JAG, 2010].

One concern is that the deep source of methane and other hydrocarbons released into the water column through the DWH oil spill may lead to emergent hypoxia in the Gulf of Mexico, comparable to, or larger than, the scale of the "Dead Zone" observed in the coastal waters (see supplemental material for background). Microbial oxidation of the hydrocarbons is hypothesized to cause significant consumption of dissolved oxygen in the water column. Another concern raised about the deep plumes is that they are harder to physically intercept than a surface slick (which can be substantially contained by booms, skimmed, burned, etc.), raising the concern that the "deep oil" may re-surface at some location remote from the spill site.

This study presents results from a numerical study that considers only the dissolved and neutrally buoyant material retained within the water column. This is an assessment of dispersal and decay mechanisms, and not a forecast and does not address the evolution of surface slicks or floating oil which are the target of tactical response modeling and clean-up activity. We examine the potential for a far-field impact of the deep material, particularly with regard to whether the deep material might exit the Gulf of Mexico. We also examine the varying lifetimes of the plumes depending on the depth of insertion and assess the impact on dissolved oxygen in the vicinity of the plumes. We find that, when the ocean circulation and microbial oxidation rates are taken into account, the interior ocean hypoxia or toxic concentrations of dissolved oil arising from the Deepwater Horizon blowout are likely to be locally significant but regionally confined to the northern Gulf of Mexico.

Methodology

The essence of our approach is to add passive tracers, subject to simple decay laws, to a climatologically-forced ocean-only model. The ocean model is a 49-layer isopycnal model configured for global simulation with a $1/8^\circ$ Mercator resolution, forced by climatology superimposed with artificial high-frequency "weather" [Griffies et al., 2009].

Each plume is modeled by a pair of passive tracers injected into the grid cell horizontally spanning the DWH site (28.737°N , 88.387°W). The passive tracers do not alter the density (which is appropriate at low enough concentrations). There is no differential rising of the oil tracer after it is introduced. The passive tracers are transported by the resolved and parameterized flow and are subject to the same parameterized vertical and lateral mixing as would apply to salinity. The explicit vertical mixing is the only mechanism that can allow vertical migration of tracers across isopycnals.

The first of the pair of tracers is conserved (non-decaying) while the second undergoes a simple decay to approximate the biological consumption of hydrocarbons. The decay time-scale, R^{-1} , is temperature-dependent with

$$R^{-1} = 12 \text{ days} \times 3^{-(T-20^\circ\text{C})/10^\circ\text{C}}, \quad (1)$$

which is broadly consistent with the studies reviewed in Atlas et al. [1981]; (1) gives $R^{-1} = 62$ days at 5°C and 7 days at 25°C . The timescales represented by (1) reflect both the time required for the dissolved oil to be colonized by microbes, as well as the rates with which some of the more refractory compounds within the oil are metabolized. More recent studies support the idea that decay should have a significant temperature dependence and give decay rates that are of a comparable magnitude (e.g., Venosa and Holder [2007]). These decay rates are broadly consistent with the the natural seepage rate into the Gulf of Mexico (2900 barrels per day, hereafter bpd) and observed background concentration, of order 10 parts per trillion [NRC, 2003]. In practice, the variations of temperature along a layer are small enough that the decay rate can be considered constant for each plume. The purpose of using a pair of tracers (decaying and non-decaying) is that it allows us to easily compute the consumption by a simple difference, as well as illustrate the role of decay in determining the lateral extent of plumes.

An analysis of a possible upper bound on the potential supply of oil to the whole interior, as well as to individual plumes at depth and in the mixed layer, is provided in the supplemental materials. We argue that an interior supply of order 10,000 bpd is consistent with all cited estimates although the error estimate varies from 5,100 bpd to 15,800 bpd. Each numerical experiment uses the same 10,000 bpd as the supply of oil to each simulated oil plume, with the intent of over-estimating the extent of any one plume but also allowing comparison between the plumes at different depths. The supply of oil to the plumes starts on 20 April 2010 and is held constant in time until it is stopped on 31 August 2010 and is a point source in space, even for the mixed layer plume, in the grid cell immediately above the location of the DWH leak. We consider one particular realization in which the Loop Current Eddy is in a broadly similar stage of separating from the contiguous Loop Current as appeared to be the case in June 2010. The simulations go for a full year.

When estimating the consumption of oxygen within the water column due to the blowout, the oxidation of methane must be accounted for. In terms of carbon supply to the water column, methane is likely to be

the biggest contributor since essentially all of it dissolves before reaching the surface. It is estimated that the flow of methane from the well is 40% that of the oil by mass. We thus use 2,400 tons/day of methane (the mass equivalent of 18,000 bpd of oil; see the supplemental materials). We assume the same consumption rate for methane as for oil.

Results

We present all of our results as comparisons between scenarios within the context of the model, since our purpose here is to illustrate the role of dispersal and decay mechanisms. We consider five plume scenarios by injecting 10,000 bpd of oil 1) into the mixed layer, 2) into the isopycnal layers that are approximately 300 m deep, 3) 700 m deep, 4) and 1100 m deep, and 5) uniformly with depth. We will refer to these plumes as "mixed layer", "thermocline", "mid-depth", "deep" and "uniform", respectively. For the four vertically localized plumes, the temperature-dependent decay time scales from (1) are approximately 9, 28, 53 and 60 days, respectively.

Oil is toxic or mutagenic at concentrations varying from 10's of parts per billion (ppb) to 10's of parts per million (10 ppm) depending on the organism in question [NRC, 2005]. We contour the column peak concentration in factors of 10 starting at 1 ppb in Fig. 1 for the model date 1 September 2010. The deep plume (Fig. 1d) has the highest peak inventory and the smallest areal extent because the currents are weakest and the decay is slowest. The currents become stronger moving up the water column and so the extension of the plume at each depth becomes greater. However, the mixed layer plume (Fig. 1a), for which the currents are the strongest, has less extension than the thermocline plume (Fig. 1b) because the decay time scale is so much shorter (9 days for the mixed layer versus 23 days for the thermocline).

The mixed layer plume (Fig. 1a) is more concentrated than the deeper plumes (Figs. 1b-d) because it is thinner (of order 10-25 m). The uniform plume (Fig. 1e) is much less concentrated than the isolated plumes, simply because it is spread throughout the entire water column (a dilution of order 100 m:1500 m with respect to other plumes). The vertical extent of the isolated plumes is mostly correlated with the layer thickness (of order 70-110 m) and the parameterized vertical mixing does not significantly diffuse the plumes in the vertical on the month time scale (not shown). The finite vertical resolution of the numerical model provides a minimum thickness for the plumes (i.e. the thickness of the isopycnal layer). Our decision to use a point source, rather than specify a vertical structure for the input, is based on a lack of detailed understanding of the termination process of the turbulent plume phase of an oil leak. The most defensible vertical plume scale is that of the mixed layer, whose scale is primarily determined by physical processes that are represented credibly in the model. The distribution of the column inventory of dissolved oil (shown in the supplementary material) is broadly similar to the peak concentrations (shown in Fig 1), but is largely independent of the exact choice of vertical plume scales. This similarity suggests that the main findings of this study are not especially sensitive to the choice of the vertical scales of the interior plumes.

The role of decay is made apparent by comparing Fig. 1a with Fig. 1f, which shows a mixed layer plume of non-decaying oil. The large areal extension of the non-decaying plume is indicative of the strong surface currents. We note that potentially significant levels of the non-decaying tracer (1 ppb) do reach into the Florida straits and Gulf Stream by mid-summer (consistent with passive tracer simulations carried out at NCAR [S. Peacock and M. Maltrud, pers. comm.]), while the decaying tracer (Fig. 1a) remains regionally confined to the northern Gulf of Mexico.

The oxygen (O_2) consumption is calculated using the oxidation of octane ($2C_8H_{18}+25O_2 \rightarrow 16CO_2 + 18H_2O$) and for the deep plume only we also include the oxidation of methane ($CH_4+2O_2 \rightarrow CO_2 + 2H_2O$). Fig. 2 shows the percentage draw-down of dissolved O_2 relative to the climatological values. The areal extent of any significant O_2 consumption is smaller than the extent of toxic concentrations for all plumes. Ignoring the role of methane, the three shallowest plumes have peak draw-downs of order 30-35% which is not sufficient to lead to hypoxia (here defined as dissolved O_2 concentrations of less than 2 mg/kg), even in the vicinity of the climatological O_2 minimum. The uniform plume has the lowest draw-down (which peaks in the O_2 minimum, not shown) and the deep plume has a draw-down peaking at 80% which is not quite sufficient to reach hypoxia. However, when methane is included in the calculation of O_2 consumption within the deep plume, the draw-down far exceeds 100% with an approximately 1,330 km² region of hypoxia. Our model's ability to exceed 100% draw-down is due to the lack of an interactive biogeochemistry model which would otherwise shut down the consumption of oil and methane when the O_2 is depleted, but also allows the results to be scaled for weaker sources. Fig. 3 shows the time series for the peak draw-down and area of hypoxia for the deep plume with methane. The peak draw-down of dissolved O_2 begins to ease shortly after termination of the oil leak (as does concentration, not shown) due to continued dilution. However, the area of hypoxia continues to grow due to lateral mixing, so long as the localized draw-down exceeds the hypoxia threshold, reaching a maximum three months after the leak stops.

Discussion

An idealized model of dissolved oil and suspended oil droplets was embedded into a climate-scale ocean general circulation model and used to assess the possibility of far field impact of the deep underwater oil plume(s) observed in the Gulf of Mexico following the explosion and sinking of the Deepwater Horizon oil rig on 20-22 April 2010. The model assumes a temperature dependent decay of oil, representing the microbial oxidation of oil. The simulated underwater oil plumes do not extend beyond the northern Gulf of Mexico, despite the strong ocean currents associated with the loop current. Significant concentrations of oil in the Florida Straits and Gulf Stream only arise when decay is not taken into account. In the decaying-oil simulations, the restricted extent of the mixed layer plume is primarily due to the rapid decay while the deep plume (sourced at a few hundred meters above the bottom) is even more restricted due to the much weaker currents at depth.

Oxygen (O_2) depletion is dominated by the decay of dissolved methane, which in this model is all incorporated into the deepest simulated plume, and has the potential to lead to regions of hypoxia in the same regions where the oil concentrations are toxic. The hypoxic regions are restricted to regions within a few hundred km of the oil/methane source, and depths of ~1000-1300 m. The mixed layer and mid-column plumes do not reach hypoxic levels, primarily because no methane reaches these layers. Concomitant with the depletion of O_2 during the conversion of hydrocarbons into CO_2 is an ocean acidification impact. As the anticipated CO_2 production is limited by the availability of O_2 , acidification impacts (e.g., undersaturation of aragonite and calcite) may be analogous to natural low- O_2 areas of the deep Pacific.

We used a point source for the plumes in both the horizontal and vertical directions. Dissolution and mixing of surface oil into the mixed layer is likely to be a laterally broader source than represented here, but we do not think this detail would greatly change the concentrations or inventories. However, the vertical scale of the plumes is initially determined by the vertical resolution of the model (of order 70-110

m at the deep plume depths) and vertical mixing processes act relatively slowly to broaden the Gaussian width of the plume by of order 100 m over ten months. In reality, the vertical scale of the plume is initially set by the processes that lead to the transition of the vertically entraining plume into a layer of more slowly drifting particles and bubbles. A vertical broadening of the simulated source would lead to lower local concentrations (not column inventory) and a lessening of oxygen draw-down.

We must emphasize that the results have no bearing on the evolution of surface slicks originating near the spill site. None of the simulations showed any indication that the deep plumes of dissolved oil could appear at the surface before decaying.

We have shown the simulated plumes on an essentially equal footing, supplying equal amounts of oil to each. In all likelihood, only the deep plume, mixed-layer plume and uniform plume will be realized and if they were to co-exist, the sum of the supply rates would match the individual plume supply used here. In such a scenario, the local concentrations would be reduced although the distribution of column inventories would be a normalized combination of the distributions obtained here.

The use of the column supply as a source for each simulated plume and the assumption of a point source in the vertical, both act to overestimate the concentrations of oil and draw-down of oxygen. Thus, we expect the simulated plumes shown here provide an upper bound on the severity of impacts.

The sensitivity to the state of the ocean was not examined here, although a second simulation with a loop current in a slightly different phase of separating showed very similar results (not shown). Chang and Oey (personal communication) use drifting particles in the context of a higher resolution regional model, using an ensemble of runs and data-assimilated initial conditions. They conclude that very few drifters at the surface and in the mid-column (~800 m) pass through the Florida Straits. We find their distribution of drifters to be in broad agreement with scales of the simulated oil plumes shown here.

We have assumed that all of the simulated oil is labile. We expect that this is a reasonable assumption for the dissolved component of the plume, but may be inappropriate for some fraction of the suspended material (bubbles and particles). A linear combination of the non-decaying and decaying tracer plumes (e.g. Figs. 1a and 1f) would suffice to represent such a composition, were the proportions known. However, the refractory component would have to constitute a significant fraction to change the results shown, since the contour intervals are logarithmic.

Based on the simulations presented here, even with all caveats taken into account, we find that potentially toxic concentrations of dissolved oil are localized to within about 100-200 km of the vicinity of the leak. Significant dissolved oxygen consumption is found when methane is considered for the deepest plume, with a total area of potential hypoxia limited to about a tenth the area of the "dead zone" on the shelf, but with an estimated volume of similar magnitude. The resulting regions of oxygen depletion are expected to be confined to the vicinity of the leak, but last longer than the toxic regions, with a peak oxygen draw-down delayed a few months from when the source is stopped.

Acknowledgments

The authors thank Sonya Legg, Charles Stock and Stephen Griffies for comments on drafts of this article, and Steve Jayne and an anonymous reviewer for thoughtful reviews. Although released by NOAA, the information in this paper does not reflect, represent, or form any part of the support of the policies of NOAA or the Department of Commerce. Further, release by NOAA does not imply that NOAA or the Department of Commerce agree with the information contained herein.

References

Atlas, R. M. (1981), Microbial degradation of petroleum hydrocarbons: an environmental perspective. *Microbial Reviews*, 45, 180-209.

Griffies S.M., and 23 co-authors (2009), Coordinated ocean-ice reference experiments (COREs). *Ocean Modelling*, 26, 1-46, doi:10.1016/j.ocemod.2008.08.007.

JAG (2010), Report of the Joint Analysis Group,
http://www.noaa.gov/sciencemissions/PDFs/JAG_Report_1_BrooksMcCall_Final_June20.pdf

National Research Council (2003), *Oil in the Sea III: Inputs Fates and Effects*. National Academy Press, 280 pp. ISBN 0-309-50551-8

National Research Council (2005), *Understanding Oil Spill Dispersants: Efficacy and Effects*, National Academy Press, 396 pp. ISBN 0-309-54793-8

Venosa, A. D., and E. L. Holder (2007), Biodegradability of dispersed crude oil at two different temperatures. *Marine Pollution Bul.*, 54, 545-553.

Figures

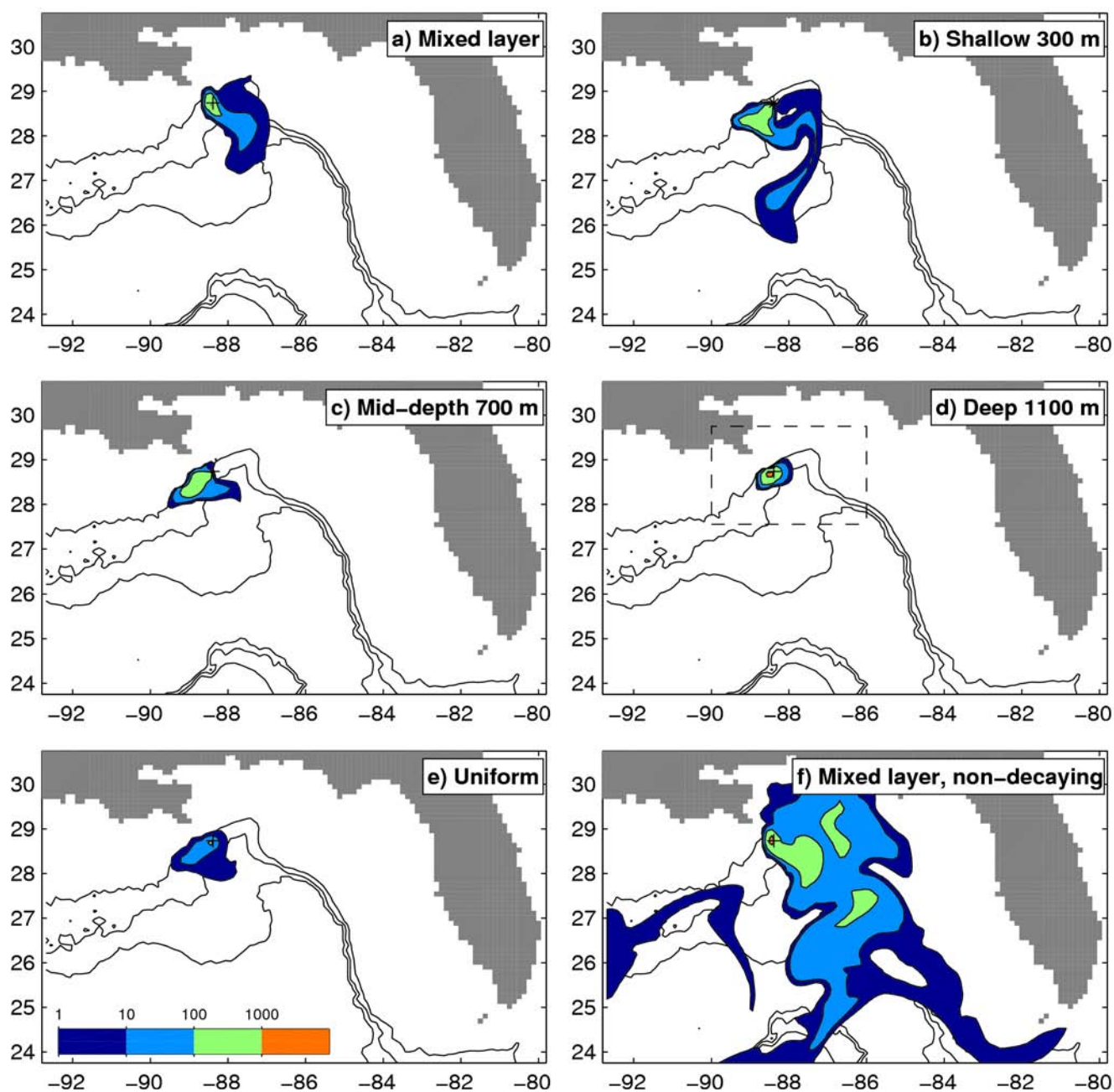


Figure 1: Peak concentration of dissolved oil (in color) within the water column, in parts per billion (ppb), on 1 September 2010 for plumes originating from a point source of 10,000 bpd at different depths. Bathymetry is contoured with a 1000 m interval. The peak concentrations for each panel are 1010, 250, 380, 1950, 190 and 1660 ppb, respectively. The mixed layer has the highest concentrations primarily because the mixed layer plume is thinner (of order 5-30 m) than the deeper plumes (of order 200-300 m thick) or the uniform plume, which is spread throughout the water column. The dashed box in panel d indicates the sub-domain plotted in Fig. 2.

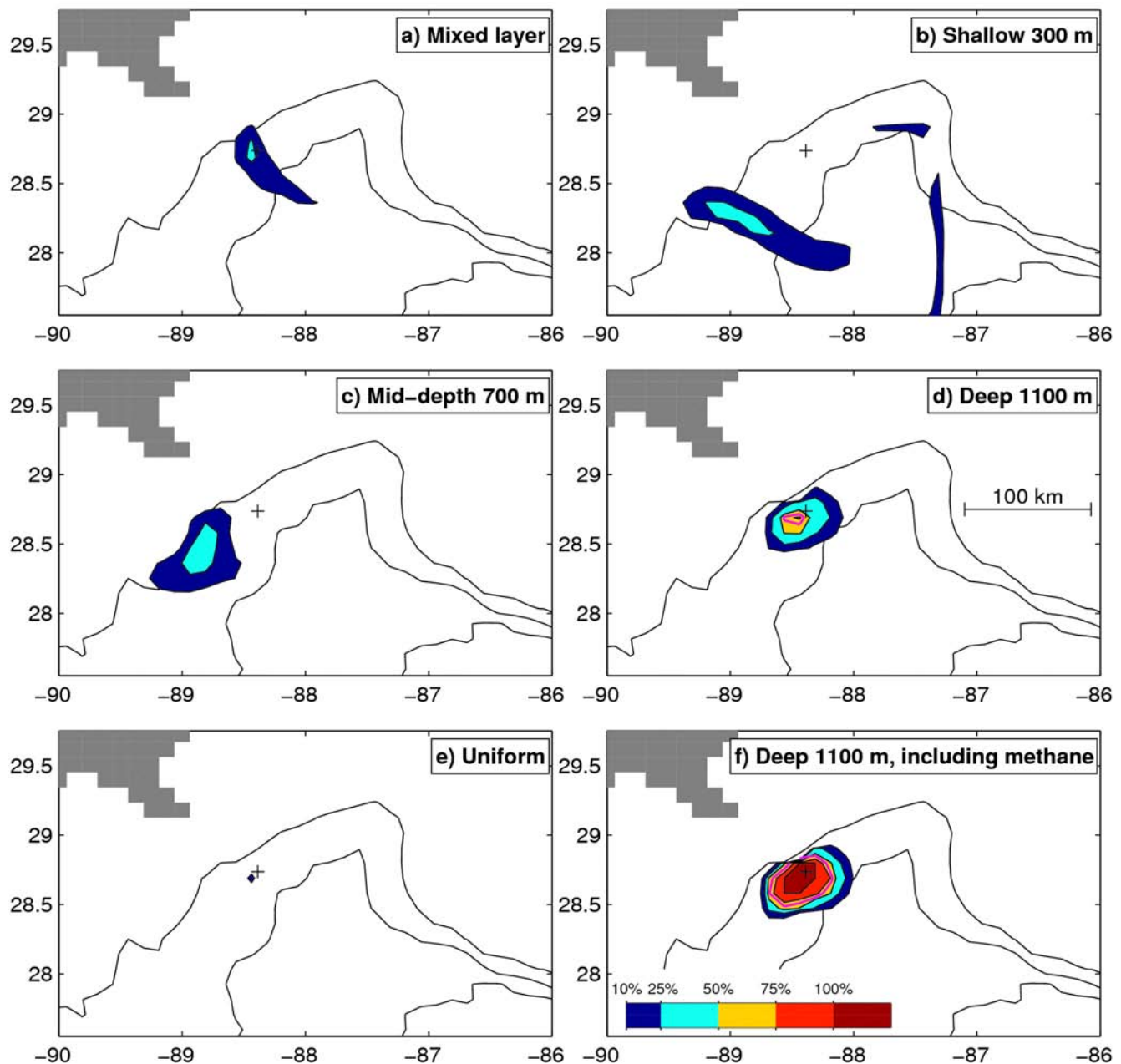


Figure 2: As for Fig. 1a-e but showing the dissolved oxygen deficit (in color) as a percentage draw-down from climatological dissolved oxygen at each depth, in the sub-domain indicated in Fig 1d. The red contour indicates the hypoxic region (panels d and f). The significant areal extent of oxygen deficit is smaller than the areal extent of potentially toxic water (Fig. 1). The three shallowest plumes (a, b and c) have peak values in the range of 30-35%. The deep plume (d) has a peak draw-down of 80% while the uniform source leads to a peak draw-down of 12% near the climatological oxygen minimum. For plumes a-e, methane oxidation is not included and none of these plumes reach hypoxic levels. Panel f shows the deep plume including a 2,400 ton/day source of methane (compare to panel d with no methane) with peak values in excess of 200% implying significant potential for hypoxia.

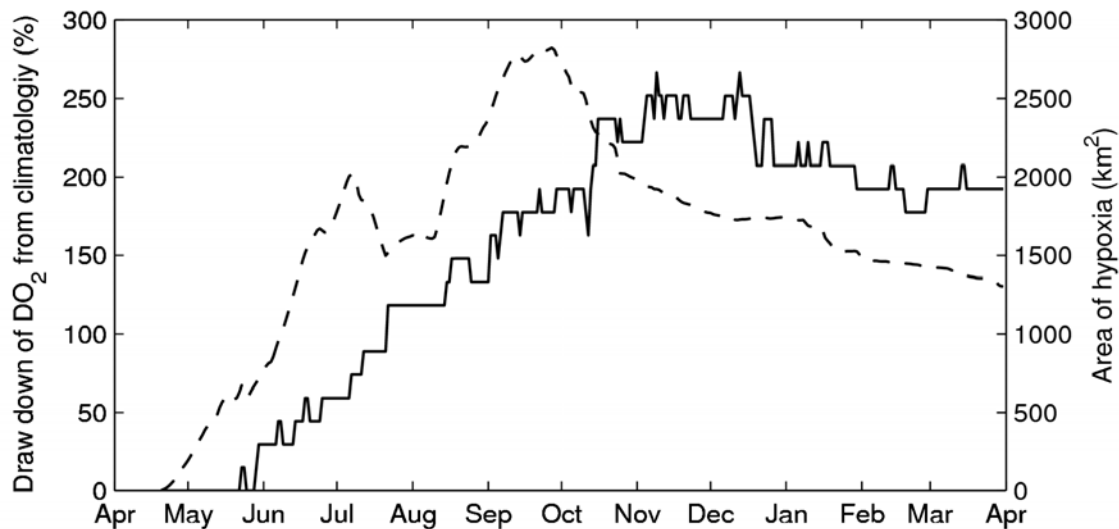


Figure 3: Time series of peak draw-down of dissolved O₂ (dashed) for the deep plume including methane (Fig. 4f) and the approximate area of hypoxia (solid). The discrete nature of the area time series is due to the relatively small area compared to the size of a grid cell in the numerical model. The peak O₂ draw-down begins to relax within a few weeks of terminating the oil leak (here 31 August 2010) but the extent of hypoxia continues to rise until the end of the year.

Supplemental material for "Simulations of underwater plumes of dissolved oil in the Gulf of Mexico"

Alistair Adcroft¹², Robert Hallberg²³, John P. Dunne², Bonita L. Samuels², J.A. Galt⁴, Christopher H. Barker⁴ and Debra Payton⁴

¹ Princeton University, Program in Atmospheric and Oceanic Sciences, 300 Forrester Rd, Sayre Hall, Princeton, NJ 08540-6654 email: adcroft@princeton.edu

² NOAA Geophysical Fluid Dynamics Laboratory, 201 Forrester Rd., Princeton, NJ 08540-6654

³ email: Robert.Hallberg@noaa.gov

⁴ NOAA Office of Response and Restoration, 7600 Sand Point Way NE, Seattle, WA 98115-6349

Appendix: Ocean circulation model description

The ocean model is an isopycnal model configured for global simulation with a $1/8^\circ$ Mercator resolution. It is forced with idealized climatological winds, air temperatures, precipitation and rivers, with synthetic but realistic high-frequency "weather", as prescribed in the CORE forcing [Large and Yeager, 2004; see also Griffies et al., 2009]. The model has 49 layers. The top two layers are used for the surface boundary layer and two more are used for variable-density transition layers [Thompson et al., 2002] The remaining 45 isopycnal layers track water of specified potential densities (relative to 2000 dbar pressure) or are massless. The surface boundary layer representation is a two-layer refined bulk mixed layer scheme, in which tracers are vertically homogenized, but momentum is not, allowing for Ekman shears and parameterized sub-mesoscale restratification [Hallberg, 2003; Fox-Kemper et al., 2008]. Although the model is eddy-permitting, a parameterization of eddy-stirring and thickness mixing is included to represent the unresolved sub-mesoscale eddy field. Thickness mixing coefficients are modulated by a local-resolution function [Hallberg and Adcroft, personal communication] and coupled to a two-dimensional eddy kinetic energy budget [Marshall and Adcroft, 2010] that closes the mechanical energy budget. The ocean model is ostensibly the same as the ocean components of GFDL's CM2G coupled climate model and GFDL's ESM2G Earth system model, but with a much finer horizontal resolution.

Appendix: Estimating the supply of oil to the interior

The volumetric supply for the deep plumes is highly uncertain. Oil leaks are stipulated in units of barrels per day, hereafter bpd (1 barrel is 42 U.S. gallons or approximately 0.159 m^3). The first official estimate of 5,000 bpd was announced within the first week [Article appearing in The New York Times on 26 April 2010, "Robots Work to Stop Leak of Oil in Gulf" by Campbell Robertson and Clifford Krauss]. The estimates from three independent methods were later summarized in the Flow Rate Technical Group (FRTG) report on 27 May 2010 [<http://www.doi.gov/deepwaterhorizon/loader.cfm?csModule=security/getfile&PageID=33972>] which provided two lower bounds; one of 11,000 bpd derived from a flow meter, and the other a plume team lower bound of 12,000-25,000 bpd (derived from analysis of video of the leaks). The third estimate of 12,000-19,000 bpd, from the mass balance team, was derived from estimates of surface inventory and model fitting. On 10 June 2010, the FRTG revised the plume team estimate to 25,000-30,000 bpd and the mass balance team to 12,600-21,500 bpd [press release by Admiral Allen and Dr. McNutt, 10 June 2010, <http://www.doi.gov/news/pressreleases/>]. All these estimates apply to the leak prior to the cutting of the broken riser pipe. On 15 June 2010, the FRTG plume team estimated the flow rate after the cutting of the riser pipe to be 35,000-60,000 bpd although for much of the period following the cut, some of the oil was being collected directly from the well head at 15,000 bpd [press announcement by Secretary Chu, Secretary Salazar and Dr. McNutt, 15 June 2010, <http://www.doi.gov/news/pressreleases/>]. The point here is that there is a great deal of uncertainty in flow rate estimates. Table 1 summarizes these estimates and in the bottom row shows our calculation of oil derived material that could be retained by the interior water column (i) accommodating the difference between the leak (b) and the surface (s). The error bar for the interior supply, i , in the inferred recent estimates (cases 1 and 2) is large, primarily because there are no independent estimates of surface supply, s . We must emphasize that this calculation assumes that the mass balance team is providing an estimate of the surface supply when in fact there are adjustments and considerations made for various sinks including oil retained in the water column. This renders our calculation to be an upper bound on the

interior supply, i . Nevertheless, an interior supply of order 10,000 bpd is consistent with all estimates although the error estimate varies from 5,100 bpd to 15,800 bpd.

A mostly independent estimate of interior supply can be made by using dispersant efficacy. Here, some fraction of the leaked oil is assumed to disperse either naturally (5-10% into a deep plume and 15% from the surface [William Lehr, personal communication; NRC, 2003, 2005]) or through the addition of chemical dispersant (of which approximately 180 bpd are being used at depth and 390 bpd are being used on the surface). The dispersant can be expected to work with a ratio of 5:1 at depth (5 parts oil to 1 part dispersant), and 3:1 ratio at the surface, yielding 900 bpd and 1170 bpd of dispersed oil at depth and the surface respectively [William Lehr, personal communication]. In Table 2, the only data in common with Table 1 is the net input of oil (b) and so these calculations are essentially independent (although the mass balance team probably used similar approaches in deriving their flow estimate). The total supply to water column, i , of 7,600-10,200 bpd in Table 2, is in broad agreement with the calculation of i in Table 1. However, Table 2 specifically contains estimates of the supply to a deep and mixed layer plumes.

Appendix: Supply of methane to water column

Due to the high ambient pressures at the drill site, methane dissolves into the water column and forms clathrates rather than making its way to the surface [Kvenvolden, 1995; Brewer et al., 1997; Adams and Socolofski, 2005]. This geochemical behavior makes the role of methane in deep oil spills much different than in shallower, shelf locations where methane simply escapes to the atmosphere. In another deep-sea environment of the Juan de Fuca hydrothermal system, methane was demonstrated to oxidize extremely rapidly even at low temperature with specific rates corresponding to 0.15 per day [de Angelis et al., 1993]. In terms of carbon supply to the water column, methane is likely to be the biggest contributor since essentially all of it dissolves before reaching the surface. It is estimated that the flow of methane from the well is 40% that of the oil by mass [Associated press article "Gulf oil full of methane, adding new concerns" by Matthew Brown and Ramit Plushnick-Masti, 18 June 2010]. We thus use 2,400 tons/day of methane (the mass equivalent of 18,000 bpd of oil), shown in last row of Table 1.

Appendix: Distinction between concentration and column inventory

In contrast to peak concentration, the column inventory is robustly conserved by the model and is largely independent of choices about the exact vertical extent of the source. However, the immediate environmental impact of the presence of oil is primarily due to the toxicity of numerous constituents of crude oil. For this reason, we have shown concentrations of dissolved oil in the main article (Fig. 1). The impact on consumption of dissolved oxygen (Fig. 2) is as much a function of column inventory (supplemental Fig. 2) as local concentration, the former giving the column-integrated consumption, while the later gives the peak draw-down. The spatial distributions of column inventory (supplemental Fig. 2) mostly follow those of the peak concentration (Fig. 1), once the vertical extent of the plumes are taken into account, except in the case of the uniform plume. For the uniform plume the inventory spreads substantially due to the vigorous near-surface currents, but only the deep waters which remain near the source acquire significant concentrations. The broad consistency of the concentrations with those of the column inventories adds confidence that the results of this study are largely independent of the exact choice of impact metrics.

Appendix: Background on the Gulf of Mexico "Dead Zone"

Depletion of dissolved oxygen levels beyond the tolerance for fish and other heterotrophs (i.e. hypoxia) is found naturally in the so called shadow zones of the Eastern Tropical Pacific and Arabian Sea but in the last century such conditions are also found in the coastal zones. There are many examples where human activities have led to an increased nitrogen flux to coastal zones resulting in decreased water quality through eutrophication with increased hypoxia, increased incidence of harmful algal blooms and fish kills, decreased water clarity and general ecosystem degradation [Cloern, 2001]. In particular, the Mississippi River Basin, draining 41% of the continental U. S., has seen immense changes in its nitrogen cycle over the last century with a 20 fold increase in fertilizer application [Alexander and Smith, 1990] contributing to a nearly three-fold increase in nitrate export by the Mississippi and Atchafalaya Rivers to the northern Gulf of Mexico [Turner and Rabalais, 1991, 1994]. These changes have dramatically enhanced primary production on the continental shelf and have caused increased severity and extent of bottom water hypoxia [Turner and Rabalais, 1991, 1994; Rabalais et al., 2001]. Interannual variability in the size of this "Dead Zone" has been shown to be driven by a combination of riverine nitrogen supply as a function of climate and land use [Donner et al. 2002; 2004] and oceanographic conditions [Lohrenz et al., 1997; Scavia et al., 2003]. Its largest extent was 22,146 km² in 2006 and is characteristically about 5 m thick [Rabalais et al., 2002]. The deep source of methane and other hydrocarbons released into the water column through the Deepwater Horizon oil spill represents a very different potential form of emergent hypoxia in the Gulf of Mexico.

Supplementary References

Adams, E. E., and S. A. Socolofsky (2005), Review of deep oil spill modeling activity supported by the DeepSpill JIP and offshore operators committee, *U.S. Minerals Management Service, Project "Deep Spill" Rep. AD*, (Available from <http://www.boemre.gov/tarprojects/377.htm>)

Alexander, R. B., and R. A. Smith (1990), County-level estimates of nitrogen and phosphorus fertilizer use in the United States, 1945 to 1985, *U.S. Geol. Surv. Open File Rep.*, 90-130. (Available from <http://pubs.usgs.gov/of/1990/ofr90130/report.html>)

Brewer, P. G., F. M. Orr, Jr, G. Friederich, K. A. Kvenvolden, D. L. Orange1, J. McFarlane, and W. Kirkwood (1997), Deep-ocean field test of methane hydrate formation from a remotely operated vehicle. *Geology*, **25**, 407-410.

Cloern, J. E. (2001), Our evolving conceptual model of the coastal eutrophication problem. *Mar. Ecol. Prog. Ser.*, **210**, 223-253.

de Angelis, M. A., M. D. Lilley, and J. A. Baross (1993), Methane oxidation in deep-sea hydrothermal plumes of the endeavour segment of the Juan de Fuca Ridge, *Deep-Sea Res I*, **40**, 1169-1186.

Donner S. D., M. T. Coe, J. D. Lenters, T. E. Twine, and J. A. Foley (2002), Modeling the impact of hydrological changes on nitrate transport in the Mississippi River Basin from 1955-1994. *Glob. Biogeochem. Cycles*, **16**, 10.1029/2001GB001396.

Donner, S. D., C. J. Kucharik, and J. A. Foley (2004), Impact of changing land use practices on nitrate export by the Mississippi River. *Glob. Biogeochem. Cycles*, **18**, doi:10.1029/2003GB002093.

Griffies S.M., and 23 co-authors (2009), Coordinated ocean-ice reference experiments (COREs). *Ocean Modelling*, **26**, 1-46, doi:10.1016/j.ocemod.2008.08.007.

Fox-Kemper, B., R. Ferrari, and R. Hallberg (2008), Parameterization of mixed layer eddies. I: Theory and diagnosis. *J. Phys. Oceanogr.*, **38**, 1145-1165.

Hallberg, R.W. (2003), The suitability of large-scale ocean models for adapting parameterizations of boundary mixing and a description of a refined bulk mixed layer model. In: Müller, P., Garrett, C. (Eds.), *Near-Boundary Processes and Their Parameterization. Proceedings of the 13th 'Aha Huliko 'a*. U. Hawaii, 187-203.

JAG (2010), Report of the Joint Analysis Group, http://www.noaa.gov/sciencemissions/PDFs/JAG_Report_1_BrooksMcCall_Final_June20.pdf

Kvenvolden, K. A (1995), A review of the geochemistry of methane in natural gas hydrate. *Organic Geochemistry*, **23**, 997-1008.

Large, W., and S. Yeager (2004), Diurnal to decadal global forcing for ocean and sea-ice models: the data sets and flux climatologies. NCAR Technical Note: NCAR/TN-460+STR. CGD Division of the National Center for Atmospheric Research.

Lohrenz, S. E., G. L. Fahnenstiel, D. G. Redalje, G. A. Lang, X. Chen, and M. J. Dagg (1997), Variations in primary production of northern Gulf of Mexico continental shelf waters linked to nutrient inputs from the Mississippi River. *Mar. Ecol. Prog. Ser.*, **155**, 45-54.

Marshall, D.P. and A. Adcroft (2010), Parameterization of ocean eddies: vorticity mixing, energetics and Arnold's first stability theorem. *Ocean Modelling*, **32**, 188-204. doi:10.1016/j.ocemod.2010.02.001.

National Research Council (2003), *Oil in the Sea III: Inputs Fates and Effects*. National Academy Press, 280 pp. ISBN 0-309-50551-8

National Research Council (2005), *Understanding Oil Spill Dispersants: Efficacy and Effects*, National Academy Press, 396 pp. ISBN 0-309-54793-8

Rabalais, N. N., R. E. Turner, and W. J. Wiseman Jr. (2001), Hypoxia in the Gulf of Mexico. *J. Environ. Qual.*, **30**, 320-329.

Rabalais, N, N, R, E, Turner, W, J, Wiseman (2002), Gulf of Mexico Hypoxia, a.k.a. "The Dead Zone", *Ann. Rev. Ecol. Systematics*, **33**, 235-263.

Scavia, D., N. N. Rabalais, R. E. Turner, D. Justic, and W. J. Wiseman (2003), Predicting the response of Gulf of Mexico hypoxia to variations in Mississippi River nitrogen load. *Limnol. Oceanogr.*, **48**, 951-956.

Thompson, L., K. A. Kelly, D. Darr, and R. Hallberg (2002), Buoyancy and mixed-layer effects on the sea surface height response in an isopycnal model of the North Pacific. *J. Phys. Oceanogr.*, **32**, 3657-3670.

Turner, R. E., and N. N. Rabalais (1991), Changes in Mississippi River water quality this century. *Bioscience*, **41**, 140-147.

Turner, R. E., and N. N. Rabalais (1994), Coastal eutrophication near the Mississippi river delta. *Nature*, **368**, 619-621.

Tables

Source of data:	FRTG 10 June 2010 report	FRTG 15 June 2010 report (case 1)	FRTG 15 June 2010 report (case 2)	FRTG 15 June 2010 report (case 3)
Flow rate at bottom (f)	27,500±2,500 bpd	47,500±12,500 bpd	47,500±12,500 bpd	47,500±12,500 bpd
Collected oil from well head (c)	n/a	15,000 bpd	15,000 bpd	15,000 bpd
Net input at bottom of water column (b=f-c)	27,500±2,500 bpd	32,500±12,500 bpd	32,500±12,500 bpd	32,500±12,500 bpd
Apparent source to surface (s)	17,000±4,500 bpd (s/b=0.618±0.174)	17,000±4,500 bpd (assuming no change in absence of new data)	20,100±9,600 bpd (assuming same ratio s/b in absence of new data)	22,000±13,500 bpd (calculated as s=b-i)
Potential supply to interior water column (i=b-s)	10,500±5,100 bpd	15,500±13,300 bpd	12,400±15,800 bpd	10,500±5,100 bpd (assuming no change in absence of data)
Flow of methane (g=2/3 x 0.133 b) using 133 kg/barrel	2,400±450 ton/day	2,900±1,100 ton/day	2,900±1,100 ton/day	2,900±1,100 ton/day

Table 1: Summary of calculations of the potential supply of oil material to the interior water column from the *Deepwater Horizon* spill. FRTG 10 June 2010 estimates provide an independent estimate of the source to surface, s, but subsequent to the cutting of the broken riser pipe we are obliged to estimate "s" and associated errors. We consider three cases: case 1 where the supply to the surface is assumed unchanged since before the cut; case 2 where the proportion between surface and interior is assumed unchanged; and case 3 where the supply to the interior is unchanged since before the cut.

Source of data:	FRTG 10 June 2010 report	FRTG 15 June 2010 report
Net input at bottom of water column (b from Table 1)	27,500±2,500 bpd	32,500±12,500 bpd
Naturally dispersed at leak (nd=5%-10% of b)	1,375-2,750 bpd	1,625-3,250 bpd
Chemically dispersed by 180 bpd of dispersant (cd=5:1 ratio)	900 bpd	900 bpd
Total supply to deep plume (d=nd+cd)	2,275-3,650 bpd	2,525-4150 bpd
Naturally dispersed at surface (ns=15% of b)	4,125 bpd	4,875 bpd
Chemically dispersed by 390 bpd of dispersant (cs=3:1 ratio)	1,170 bpd	1,170 bpd
Total supply to mixed layer plume (m=ns+cs)	5,295 bpd	6,045 bpd
Total supply to water column (i=d+m)	7,570-8,945 bpd	8,570-10,195 bpd

Table 2: Summary of calculation of interior water column supply rates of oil material based on dispersion efficacies. The only data in common with Table 1 is the net input of oil (b) and so these calculation are essentially independent. The critical inputs to this calculation are the supply of dispersant (180 bpd at depth and 390 bpd at the surface), the dispersant ratios (5:1 and 3:1, respectively) and the fraction of naturally dispersed oil (5-10% at depth and 15% at surface). The total supply to the water column (i) is in broad agreement with the calculation of i in Table 1.

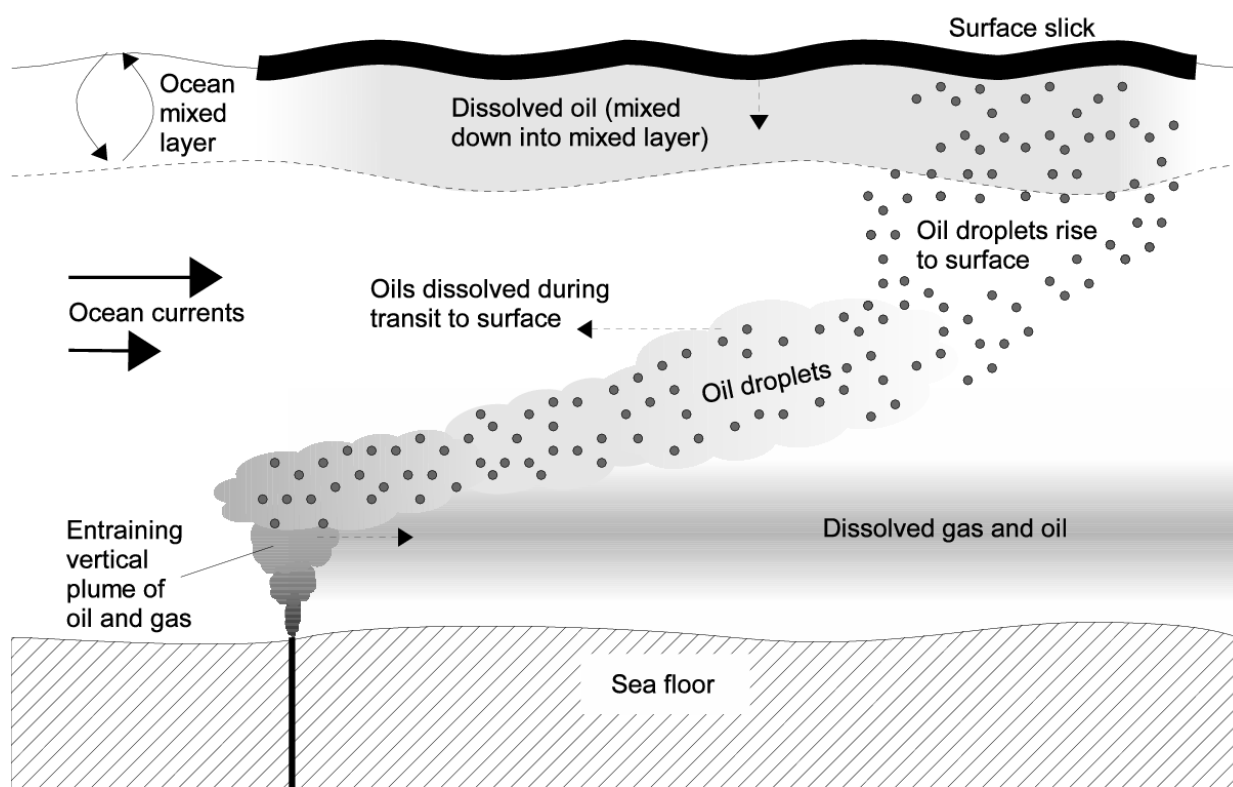
Figures

Figure 1: Schematic of a deep oil leak. This study focuses on the dissolved and suspended materials rather than the rising and floating material (slick). The three principle sources of dissolved material are a) at the termination of the vertical plume where methane is mostly dissolved, b) the dissolution of oil from surface material as it is being perpetually stirred down into the mixed layer, and c) the dissolution of material as it transits the water column.

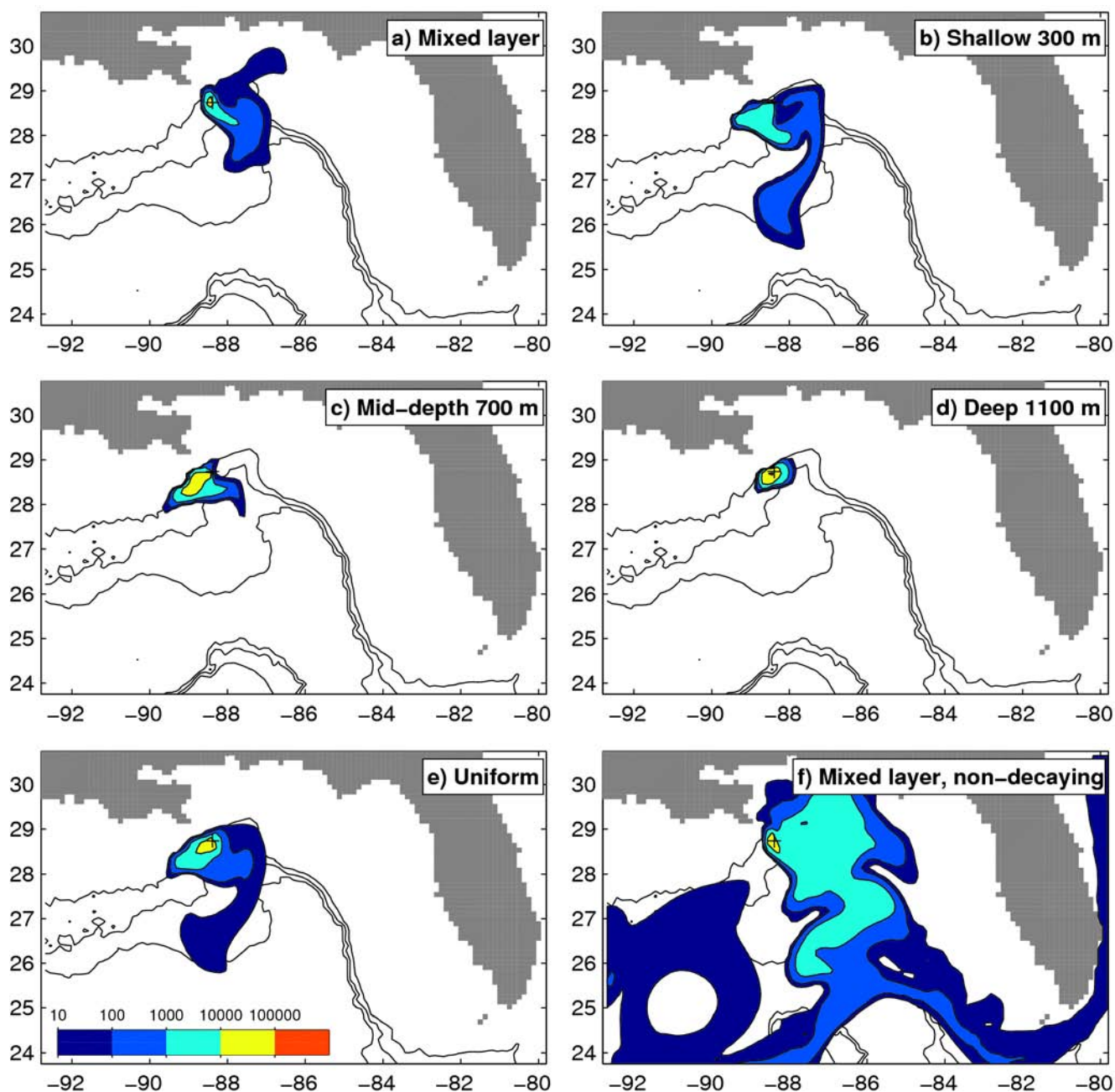


Figure 2: Column inventory of dissolved oil in liters/km² (in color) on 1 September 2010 for plumes originating from a point source of 10,000 bpd at different depths. Shown are plumes originating from a) the mixed layer (with a peak value of 21,200 l/km²), b) at 300 m depth (with a peak value of 8,100 l/km²), c) at 700 m depth (with a peak value of 27,600 l/km²), d) at 1100 m depth (with a peak inventory of 135,000 l/km²), and e) a vertically uniform source (with a peak inventory of 91,700 l/km²). Panel f) shows the mixed layer plume for a non-decaying oil (with a peak inventory of 35,000 l/km²) to be compared with panel a).